Covalent Organic Frameworks

International Edition: DOI: 10.1002/anie.201913975
German Edition: DOI: 10.1002/ange.201913975

Acid Exfoliation of Imine-linked Covalent Organic Frameworks Enables Solution Processing into Crystalline Thin Films

*David W. Burke, Chao Sun, Ioannina Castano, Nathan C. Flanders, Austin M. Evans, Edon Vitaku, David C. McLeod, Robert H. Lambeth, Lin X. Chen, Nathan C. Gianneschi, and William R. Dichtel**

Abstract: *Covalent organic frameworks (COFs) are highly modular porous crystalline polymers that are of interest for applications such as charge-storage devices, nanofiltration membranes, and optoelectronic devices. COFs are typically synthesized as microcrystalline powders, which limits their performance in these applications, and their limited solubility precludes large-scale processing into more useful morphologies and devices. We report a general, scalable method to exfoliate two-dimensional imine-linked COF powders by temporarily protonating their linkages. The resulting suspensions were cast into continuous crystalline COF films up to 10 cm in diameter, with thicknesses ranging from 50 nm to 20 μm depending on the suspension composition, concentration, and casting protocol. Furthermore, we demonstrate that the film fabrication process proceeds through a partial depolymerization/repolymerization mechanism, providing mechanically robust films that can be easily separated from their substrates.* ■■ *Shortened to character limit.* ■■

Introduction

Covalent organic frameworks (COFs) are an emerging class of porous crystalline polymers constructed from combinations of geometrically compatible monomers that are capable of polymerizing into two- or three-dimensional networks.[1–3] These materials have attracted significant attention over the past decade due to their high stability,[4] accessible pores, and tunable functionality[5] that demonstrate promise for applications including energy[6,7] and gas storage,[8] catalysis,[9,10] and membrane-based separation.[11–14] However, most reported syntheses produce COFs as insoluble microcrystalline powders, a morphology that precludes many of these uses.[15] Recent efforts have been directed towards fabricating 2D COF thin films, a morphology ideal for applications requiring rapid mass transport through the pores.[16,17] In particular, large-area films with precisely defined thickness and oriented crystalline domains are ideal.[17]

Three main strategies have been developed to access COF thin films. The first is solvothermal synthesis, in which the COF is grown directly on a solid support.[17–21] This method produces highly crystalline films, with pores sometimes oriented perpendicular to the substrate,[18,22] but suffers from numerous disadvantages, including difficult scale-up, lack of generality across substrate types, production of powder products in addition to the film, and the inability to transfer films between supports.[16] The second is interfacial polymerization, in which the monomers or catalyst are dissolved separately in two immiscible solvents such that COF formation occurs at the interface.[11,23,24] This strategy provides freestanding films, but thickness control requires significant reoptimization for every network, and films with poor or no crystallinity are often obtained, especially when they are thinner than 50 nm.[24,25] Finally, a third method, exfoliation and reconstitution of COF powders, has been explored.[26–29] This strategy is highly desirable because it provides a direct route to the film morphology from abundant microcrystalline powders, which are simpler to synthesize, and the film dimensions can be precisely tuned by changing the suspension concentration and substrate surface area.[16]

Although numerous COF powder exfoliation methods have been reported,[15,30–37] very few of these studies demonstrate the ability to reconstitute the resulting nanosheets into large-area COF films.[26–29] Most reported methods involve either sonicating[27,30–32,35] the powders in organic solvents or mechanically grinding[15,34,36] the powders prior to dispersion, but due to challenges with re-aggregation and sedimentation at high concentrations,[33,38,39] these strategies typically produce dilute suspensions ($\leq 0.2\ mg\,mL^{-1}$) that are not conducive to large-scale film fabrication.[27,30–32,36] Although Tsuru and co-workers demonstrated that thin films can be

[*] D. W. Burke, Dr. C. Sun, I. Castano, N. C. Flanders, A. M. Evans, Dr. E. Vitaku, Prof. L. X. Chen, Prof. N. C. Gianneschi, Prof. W. R. Dichtel
Department of Chemistry, Northwestern University
Evanston, IL 60208 (USA)
E-mail: wdichtel@northwestern.edu
Dr. C. Sun
Present address: Max Planck Institute for Brain Research
Frankfurt am Main (Germany)
Dr. D. C. McLeod, Dr. R. H. Lambeth
U.S. Army Research Laboratory
Aberdeen Proving Grounds, MD 21005 (USA)
Prof. L. X. Chen
Chemical Sciences and Engineering Division
Argonne National Laboratory, Argonne, IL 60493 (USA)
Prof. N. C. Gianneschi
Departments of Materials Science and Engineering, Biomedical Engineering, International Institute for Nanotechnology
Simpson Querry Institute, Chemistry of Life Processes Institute
Northwestern University, Evanston, IL 60208 (USA)
Supporting information and the ORCID identification number(s) for the author(s) of this article can be found under: https://doi.org/10.1002/anie.201913975.

prepared from a dilute suspension (0.15 mg mL^{-1}) of COF-1 powder prepared through sonication in dichloromethane, the fabrication process required repeated drop-casting/drying cycles to form a continuous film, and therefore lacks scalability and practicality.[27] More recently, charge-mediated[28,29,33,37] and chemical[26,39,40] exfoliation strategies have been developed, which produce more concentrated suspensions ($\geq$ 0.5 mg mL^{-1}) that can be drop-cast to produce large-area films.[26,28,29] However, these strategies have thus far made use of intentionally incorporated functional groups that are not generalizable across broad classes of COF networks.[26,28,29,33,37,39] For example, Banerjee and co-workers demonstrated that an anthracene-based 2D COF powder could be chemically exfoliated through a Diels–Alder reaction between the anthracene units and *N*-hexylmaleimide.[26] Furthermore, Ma and co-workers synthesized a 2D COF containing cationic viologen units, such that the resulting sheets were easily separated due to electrostatic repulsion.[28]

Herein, we report a general method to exfoliate imine-linked COFs, one of the largest and most structurally diverse COF classes, by temporarily protonating their imine linkages (Figure 1 A). These suspensions were deposited onto various substrates to produce crystalline COF films with thickness ranging from 50 nm to 20 μm, depending on the suspension composition, concentration, and casting method. Films quickly delaminate from the substrate when submerged in alcohol and can be transferred to any desired support. This strategy was generalized to three imine-linked COF structures, all lacking the functional handles required for previously reported charge and chemical exfoliation methods.[26,28,29,33,37,39] Finally, we demonstrate that the acid, in combination with small quantities of water, reactivates the imine linkages for exchange as the suspension dries, which enables the COF particles to partially break down and subsequently repolymerize as the film forms. This results in highly crystalline yet mechanically robust films. These results suggest that acid-mediated exfoliation is a powerful alternative to previously reported film fabrication techniques and will enable the synthesis of the next generation of COF materials.

Results and Discussion■■Heading ok here (it was missing)?■■

Protonation of the 2D imine-linked BND-TFB COF (Figure 1 B) with excess trifluoroacetic acid (TFA) enables its dispersion in organic solvents and degrades its apparent crystallinity and porosity, yet preserves most of its imine linkages. After stirring in a mixture of acetonitrile, tetrahydrofuran, and TFA (7:3:2 *v*/*v*/*v*) overnight, the COF powder was broken up into a polydisperse suspension containing a wide range of particle sizes. The powder's color also changed from bright orange to red upon acid addition, which is consistent with protonation of the imine linkages. Analogous color changes were previously observed upon protonation of imine-linked macrocycles[41] and COFs.[42] The exfoliated solids were isolated by centrifugation, washed, and dried under vacuum overnight prior to characterization. Powder X-ray diffraction (PXRD) and nitrogen adsorption data (Figure 2 A,B) indicate that the excellent crystallinity and surface area of the starting COF powder (S_{BET} = 2120 m^2 g^{-1}) are mostly lost after acid exfoliation (S_{BET} = 5 m^2 g^{-1}). However, the Fourier-transform infrared (FT-IR) spectra of both the initial powder and the exfoliated solids (Figure 2 C) are nearly identical, (The FTIR spectra in Figure 2C look quite different) and both contain a sharp imine peak at around 1620 cm^{-1}, thus indicating that the imine-linked network is largely preserved. We hypothesize that the reductions in crystallinity and surface area are due to disordered stacking of the protonated COF sheets after acid treatment, which minimizes electrostatic repulsion. We predict that this repulsion enables their exfoliation. A similar disrupted stacking model was recently validated by Medina and co-workers, who observed a reduction in the crystallinity

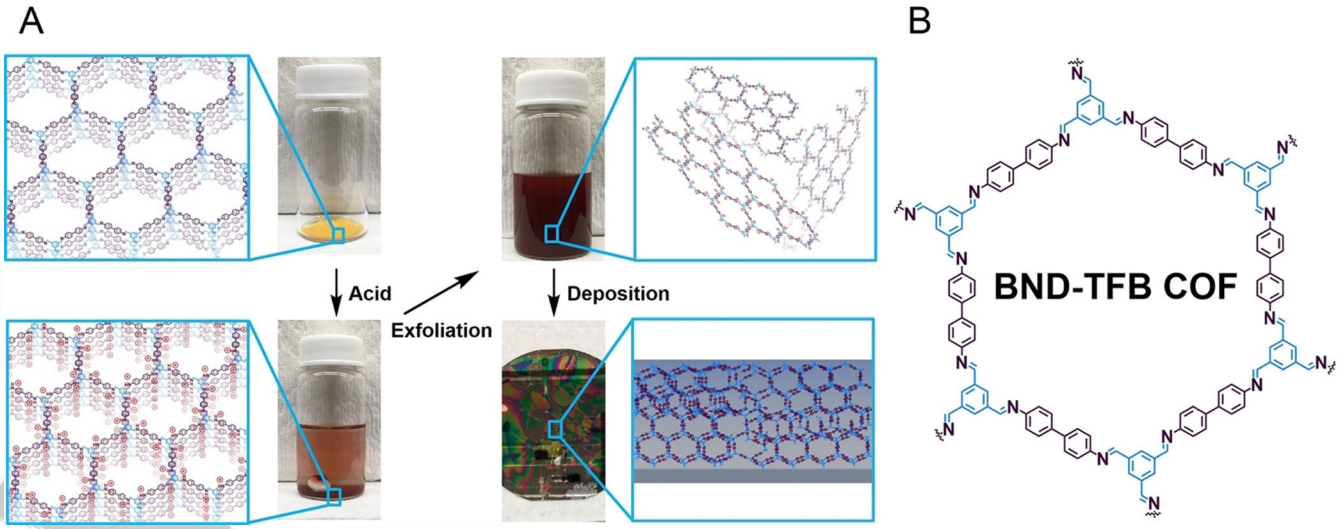

Figure 1. A) Overview of the acid-exfoliation and film-casting procedures. Protonation of imine-linked COF powders results in electrostatic repulsion between adjacent layers, which induces rapid exfoliation of the powders into thin sheets upon stirring. Suspensions of exfoliated COF sheets were deposited onto substrates and dried into thin crystalline COF films. B) Pore structure of the BND-TFB COF.

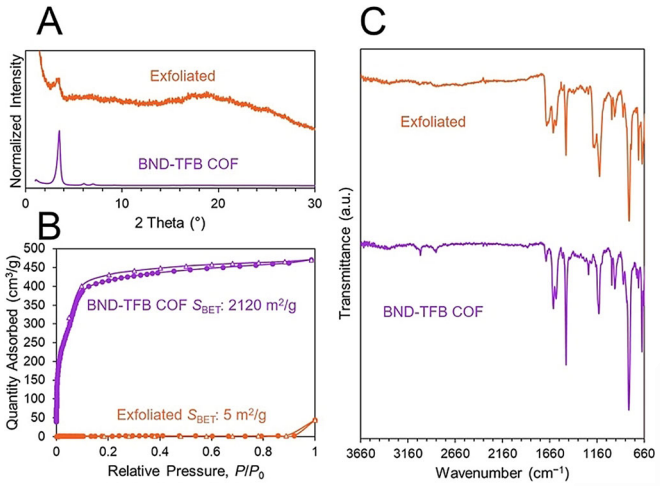

Figure 2. Characterization of BND-TFB COF powder prior to exfoliation (BND-TFB COF, purple) and after exfoliation (Exfoliated, orange). A) PXRD patterns indicate a significant loss of crystallinity upon exfoliation. B) Nitrogen adsorption (circles) and desorption (triangles) isotherms (77 K) indicate that the porosity of the as-synthesized BND-TFB COF is lost after treatment with acid. C) FT-IR spectra of each material suggest that the imine-linked network is largely conserved during this process.

and porosity of several imine-linked COF powders upon exposure to certain solvents.[43]

High-resolution transmission electron microscopy (HRTEM) and atomic force microscopy (AFM) images of drop-cast BND-TFB COF suspensions provide further evidence that the exfoliated sheets maintain their integrity and periodicity during acid exfoliation (Figure 3). HRTEM imaging revealed the presence of large (>300 nm diameter) thin sheets of crystalline COF with lattice fringes extending throughout the structures (Figure 3A, Figure S4). A fast Fourier transform (FFT) was applied to two regions of the image shown in Figure 3A, both of which reveal uniform six-fold symmetry with lattice spacings of approximately 22 Å, which closely match d_{100} of BND-TFB COF powder (Figure 3B). Some particles without lattice fringes were also observed, which may be attributed to aggregates too thick to analyze by TEM, particles that were damaged by the electron beam, or other weakly crystalline or amorphous structures produced as a byproduct of the exfoliation process. To measure the dimensions of the dispersed particles, an aliquot of BND-TFB COF suspension was deposited onto a freshly cleaved HOPG■■Please define.■■ substrate and imaged by AFM. These images revealed the presence of a wide distribution of particle sizes, the smallest of which are approximately 5 nm thick and 50 nm in diameter (Figure 3C). Particles with 50 nm thickness and greater than 1 μm diameter were also observed, with still larger aggregates visible to the naked eye, thus indicating a broad size distribution. These sizes were further confirmed by dynamic light scattering (DLS) measurements (Figure S5). Collectively, these results suggest that acid treatment disperses 2D imine-linked COF powder into a polydisperse suspension while preserving its porous, periodic structure.

When the exfoliated BND-TFB COF suspension is deposited onto a silicon wafer and allowed to evaporate in air, it dries into a uniform continuous thin film that retains some of the crystallinity and porosity of the pristine COF powder. Immediately after deposition, the suspension exhibited a red color and contained visible aggregates, but became more uniform and yellow before drying into a bright red film (Figure S6). The resulting film (400 nm thick) was imaged by AFM, which revealed an array of discrete circular particles piled into an extended structure, as expected for an assembly of 2D polymer sheets (Figure 4A). A portion of the COF film was submerged in reagent alcohol (90% ethanol, 5% methanol, 5% isopropanol) immediately after drying, and its color rapidly changed from red to yellow, which we attribute to the deprotonation of its iminium ions back to neutral imines.[41,42] Notably, the film also delaminated from

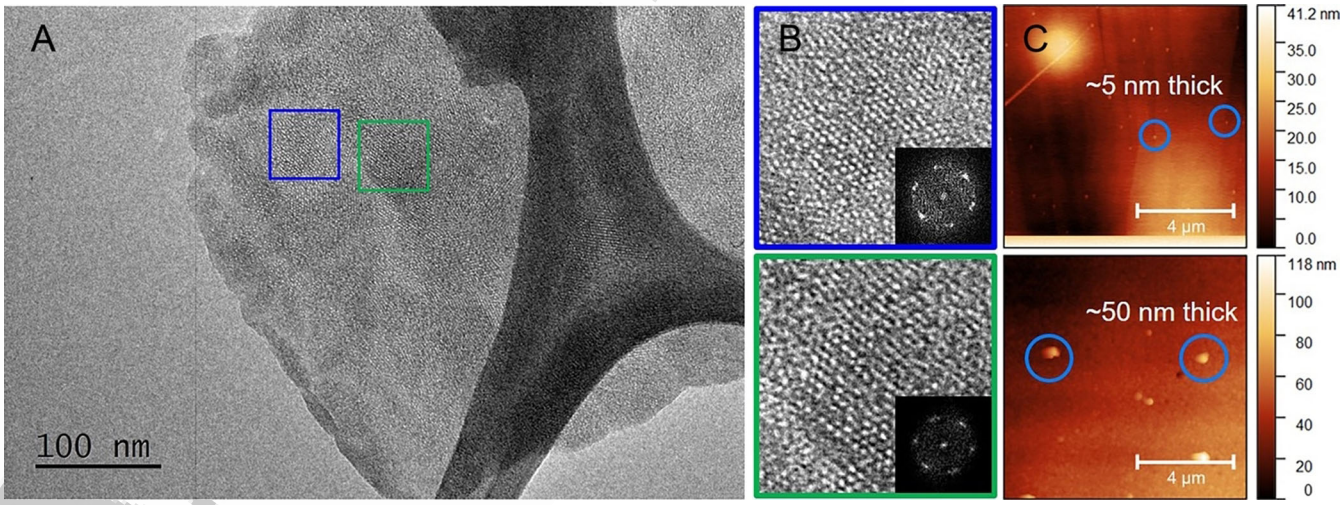

Figure 3. A) HRTEM image of an exfoliated BND-TFB COF sheet. B) Two regions of interest at higher magnification corresponding to the blue and green boxed regions of the sheet in (A). Inset: FFTs of the two high-magnification images from the two color-coded regions of interest in (B) show the predominant diffraction feature (ca. 22 Å). C) AFM images of exfoliated BND-TFB COF particles deposited onto freshly cleaved HOPG reveal a distribution of particle sizes.

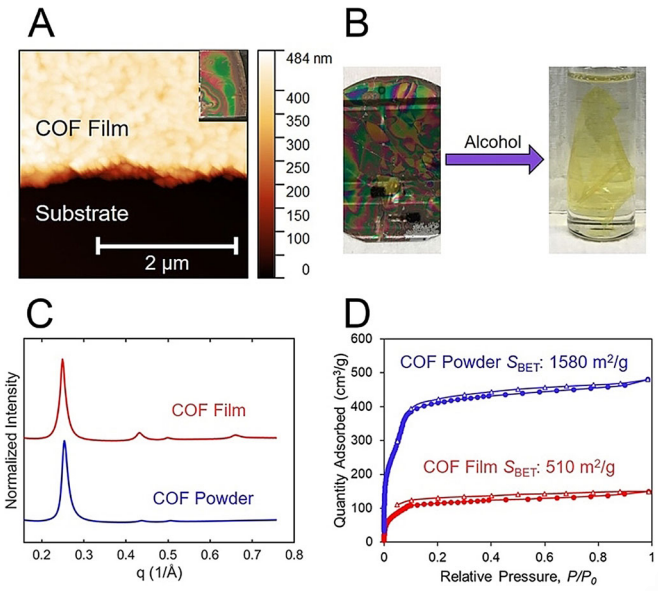

Figure 4. Characterization of BND-TFB COF films. A) AFM image of the edge of a 400 nm thick film. B) Photographs of a film before and after delamination with reagent alcohol. C) WAXS patterns of BND-TFB COF powder (blue) and a film prepared via acid exfoliation of that powder (red), both normalized at the (100) peak. D) Nitrogen adsorption (circles) and desorption (triangles) isotherms (77 K) of COF powder (blue) and a corresponding COF film (red).

the substrate, providing a freestanding COF film (Figure 4B) that could be transferred to any desired support. To evaluate the crystallinity of these freestanding films, a BND-TFB COF film (variable thickness of 2–5 μm) was packed into a capillary while wet with reagent alcohol and analyzed by synchrotron wide-angle X-ray scattering (WAXS) measurements. The film exhibited sharp diffraction peaks at the same positions as the starting COF powder, with crystalline domain sizes of 34 nm calculated by Scherrer analysis of the (100) peak for both materials (Figure 4C). Grazing-incidence wide-angle X-ray scattering (GIWAXS) measurements of a substrate-bound COF film confirmed that these crystalline domains exhibit no preferential orientation (Figure S8). Two additional freestanding BND-TFB COF thick films were activated by supercritical CO_2 drying and interrogated by nitrogen adsorption measurements (Figure 4D), revealing that the films ($S_{BET} = 510\ m^2\,g^{-1}$) retained some of the porosity of the parent powder ($S_{BET} = 1580\ m^2\,g^{-1}$). This reduction in surface area may arise from the disordered stacking of COF sheets, or regions of amorphous imine-linked polymer produced as a byproduct of the exfoliation and film casting processes.

Film thickness can be precisely controlled by modifying both the concentration of the exfoliated COF suspension and the casting technique. Suspensions ranging in concentration from 2–10 $mg\,mL^{-1}$ COF were spin-coated onto silicon wafers at various spin speeds to access continuous thin films ranging from 50–150 nm thick (Table S1, Figure S11). Meanwhile, 400 nm^{-5} μm films were prepared by drop-casting suspensions of equivalent concentrations (Figure 4A, Figure S12). Such fine control of film thickness has not been achieved by interfacial polymerization or solvothermal synthetic methods,[11,18,24] thus making this approach ideal for fabricating membranes for chemical-separation applications, where the film thickness and pore size define the performance of the material.[44–46]

Crystalline films were fabricated from two additional imine-linked COF powders (TAPB-PDA COF, Methyl COF, Schemes S2, S3), thereby establishing the generality of the method. In each case, the pristine COF powder was exfoliated through stirring and sonication in the presence of TFA. Notably, when the exfoliated TAPB-PDA and Methyl COF solids were isolated, purified, and activated by supercritical CO_2 drying, high surface areas (Figures S15, S28) and crystallinity (Figures S13, S26) were still observed. In these cases, the iminium ions were deprotonated by large volumes of methanol during the workup, as indicated by a color change from red to bright yellow.[41,42] HRTEM images of exfoliated TAPB-PDA and Methyl COF particles both contained lattice fringes with spacings of approximately 32 Å, which corresponds to d_{100} of both structures (Figures S21, S34). Exfoliated suspensions of both COFs were then drop-cast onto silicon wafers, and the resulting films were delaminated in reagent alcohol. Both exhibited WAXS signals consistent with the corresponding COF powders, thus indicating that this method can be applied to various imine-linked structures with different pore sizes (Figures S25, S38).

Nuclear magnetic resonance (NMR) spectra of exfoliated COF suspensions suggest that the imine linkages become dynamic upon exposure to air and water, and undergo partial disassembly and reassembly as the suspension dries into a uniform crystalline film. To probe the composition of the exfoliated COF suspension as it transitions from a polydisperse red mixture to a uniform yellow solution, two BND-TFB COF suspensions (2 $mg\,mL^{-1}$) were prepared in 7:3:2 [D_3]acetonitrile/tetrahydrofuran/TFA, and a known quantity of 1,3,5-trichlorobenzene was dissolved in each as an internal standard. One of the suspensions was uncapped and exposed to air until it became mostly uniform and yellow, at which point both were filtered and analyzed by ^{1}H NMR spectroscopy to determine their monomer contents (Figures S45, S46). These results indicate that, prior to air exposure, only 7% (see Section J in the Supporting Information for calculations) of the COF had been converted back into monomers, which is consistent with our previous finding that most of the imine linkages remain intact upon initial acid treatment. However, after several hours of air exposure, approximately 66% of the COF powder had depolymerized back to its constituent monomers, thus suggesting that the film crystallization pathway is highly dynamic and proceeds via a largely hydrolyzed phase. It is worth noting that the uniform yellow solution still contained a few visible aggregates, which were removed by filtration prior to collection of the NMR spectrum. Such aggregates typically dissolve during the film-casting process, so the degree of disassembly may be even greater under those circumstances. Based on these results, we hypothesized that moisture enters the suspension upon exposure to humid air, reactivating the imine linkages for exchange as the film dries. To test this hypothesis, we repeated the experiment with an equivalent BND-TFB COF suspension (2 $mg\,mL^{-1}$) containing 1% *v*/*v* H_2O and no air exposure time, which revealed a nearly identical degree of degradation (68%, Figure S47).

Furthermore, similar results were obtained with TAPB-PDA COF suspensions (Figures S48–S50, Table S3). These results, in combination with the excellent crystallinity and high surface areas of the resulting films, provide compelling evidence that water from the atmosphere facilitates an initial depolymerization of the COF network, followed by a repolymerization step to form a uniform crystalline film. We speculate that TFA is ideal for facilitating this process because it is volatile and capable of solubilizing the intermediate monomers and oligomers. Such a unique mechanism of COF film formation has not been previously reported and warrants further investigation.

By modifying the exfoliating solvent composition, solutions with COF contents as high as 25 mg mL^{-1} were prepared, providing access to large-area crystalline films up to 20 μm in thickness. Based on our NMR spectroscopy data, we hypothesized that we could bypass the depolymerization step of the film-casting process by adding water to the suspensions prior to casting. Furthermore, by breaking down some of the COF aggregates with added water, we expected that we would be able to prepare more concentrated suspensions, and therefore thicker films. Notably, when the standard exfoliating solvent (7:3:2 acetonitrile/tetrahydrofuran/TFA) was modified to contain 5% *v*/*v* H_2O, 50 mg of TAPB-PDA COF powder (Figure S39A) dissolved completely after stirring for 4 hours (Figure S39B). With less H_2O, well-dispersed COF aggregates formed a flocculent solid instead of completely dissolving. When the acetonitrile/tetrahydrofuran portion of the solvent mixture was removed, 50 mg of TAPB-PDA COF powder completely dissolved in 2 mL of TFA (5% *v*/*v* H_2O) in under 30 minutes to form a transparent red solution (Figure S39C). Films up to 50 mg in mass and around 10–20 μm in thickness were cast from TFA/H_2O solutions in glass or aluminum dishes. To efficiently neutralize all iminium ions, these thicker films were washed with alcohol followed by base (see the Supporting Information). After supercritical CO_2 drying, the films (Figure S39D) exhibited PXRD patterns equivalent to the pristine powder (Figures S40). Furthermore, they retained up to 80% of the powder surface area as confirmed by nitrogen adsorption measurements (Figure S41), as well as the characteristic FT-IR imine stretch at approximately 1620 cm^{-1} (Figure S44). These materials (S_{BET} = 1750 m^2 g^{-1}) represent some of the highest quality freestanding COF films reported to date.[11,14,24,25,47]

NMR spectroscopy measurements of COF solutions in TFA-d/D_2O reveal a COF concentration dependence on the degree of depolymerization. To probe how the roles of the acid and water change as a function of COF concentration during the film-fabrication process, and establish the generality of the depolymerization/repolymerization mechanism across solvent mixtures, two uniform TAPB-PDA COF solutions (12.5 mg mL^{-1} and 25 mg mL^{-1}) were prepared in TFA-d (5% *v*/*v* D_2O) along with a 1,4-dioxane internal standard and analyzed by ^{1}H NMR spectroscopy (Figures S51, S52). These results indicate that 57% of the COF powder in the 12.5 mg mL^{-1} suspension was converted back into the constituent monomers, while only 46% of the powder in the 25 mg mL^{-1} suspension had undergone complete disassembly. At the same time, additional aromatic peaks likely corresponding to small oligomers or forming polymers became more prevalent in the ^{1}H NMR spectrum of the 25 mg mL^{-1} suspension compared to its more dilute counterpart. Similar results were obtained for BND-TFB COF solutions in TFA-d/D_2O (Figures S53, S54, Table S5). These results suggest that the combination of TFA and water favors disassembly of imine-linked COFs at low concentration, whereas repolymerization becomes more favorable at high concentration, thus providing further evidence for the proposed mechanism. We predict that this mechanism may provide several benefits over traditional exfoliation/reconstitution strategies. First, the initial hydrolysis step limits issues with reaggregation and sedimentation that complicate solvent-mediated and mechanical exfoliation processes.[33,38,39] Second, the repolymerization step has the potential to covalently link newly forming crystalline domains, thereby providing a mechanically robust film. A more comprehensive study of this crystallization pathway is currently underway.

Conclusion

In conclusion, we demonstrated that addition of acid to 2D imine-linked COF powders enables their dispersion in organic solvents by temporarily weakening their interlayer stacking through electrostatic repulsion. The exfoliated COF suspensions were characterized by PXRD, nitrogen adsorption measurements, IR spectroscopy, TEM, and NMR spectroscopy, the results of which suggest that the imine linkages are largely maintained upon protonation but reactivated for exchange upon exposure to air and water. Furthermore, we prepared freestanding, crystalline films from three different COF powders by casting acid-exfoliated COF suspensions, and demonstrate excellent thickness control based on suspension composition, concentration, and casting technique. These results suggest that acid exfoliation can be leveraged as a powerful strategy for the solution processing of abundant imine-linked COF powders into functional devices, thereby opening up a wealth of potential applications for this class of materials that were previously inaccessible.

Acknowledgements

This research was supported by the National Science Foundation (087147-16468-01//CBET-1706219) and the Northwestern University Materials Research Science and Engineering Center (NSF DMR-1720139). D.W.B., I.C., and A.M.E. are supported by the Ryan Fellowship and the Northwestern University International Institute for Nanotechnology. I.C. is supported by the NSF Graduate Research Fellowship under grant DGE-1842165. A.M.E. is supported by the NSF Graduate Research Fellowship under grant DGE-1324585. Partial support for N.C.F. and L.X.C. is from Chemical, Biological, Geological Sciences Division, Basic Energy Sciences, US Department of Energy under Contract No. DE-AC02-06CH11357. Research is supported in part by appointments (D.M.) to the U.S. Army Research Laboratory

Research Associate Program administered by the Oak Ridge Associated Universities through a contract with the U.S. Army Research Laboratory. This work made use of the IMSERC at Northwestern University, which has received support from the Soft and Hybrid Nanotechnology Experimental (SHyNE) Resource (NSF ECCS-1542205), the State of Illinois, and the International Institute for Nanotechnology (IIN), as well as the Keck-II and SPID facilities of Northwestern University's NUANCE Center, which has received support from the Soft and Hybrid Nanotechnology Experimental (SHyNE) Resource (NSF ECCS-1542205); the MRSEC program (NSF DMR-1720139) at the Materials Research Center; the International Institute for Nanotechnology (IIN); the Keck Foundation; and the State of Illinois, through the IIN. This research used resources of the Advanced Photon Source (Sectors 5, 8, and 12), a U.S. Department of Energy (DOE) Office of Science User Facilitiy operated for the DOE Office of Science by Argonne National Laboratory under Contract No. DE-AC02-06CH11357. Portions of this work were performed at the DuPont-Northwestern-Dow Collaborative Access Team (DND-CAT) located at Sector 5 of the Advanced Photon Source (APS). DND-CAT is supported by Northwestern University, E.I. DuPont de Nemours & Co., and the Dow Chemical Company. We acknowledge Gatan Inc., Pleasanton, CA, USA for the use of the K3-IS camera installed at NUANCE.

Conflict of interest

The authors declare no conflict of interest.

Keywords: covalent organic frameworks · exfoliation · nanosheets · polymers · solution processing

[1] A. P. Côté, A. I. Benin, N. W. Ockwig, M. Keeffe, A. J. Matzger, O. M. Yaghi, *Science* **2005**, *310*, 1166 – 1170.
[2] H. M. El-Kaderi, J. R. Hunt, J. L. Mendoza-Cortés, A. P. Côté, R. E. Taylor, M. Keeffe, O. M. Yaghi, *Science* **2007**, *316*, 268 – 272.
[3] M. S. Lohse, T. Bein, *Adv. Funct. Mater.* **2018**, *28*, 1705553.
[4] A. M. Evans, M. R. Ryder, N. C. Flanders, E. Vitaku, L. X. Chen, W. R. Dichtel, *Ind. Eng. Chem. Res.* **2019**, *58*, 9883 – 9887.
[5] C. S. Diercks, O. M. Yaghi, *Science* **2017**, *355*, eaal1585.
[6] Z. Lei, Q. Yang, Y. Xu, S. Guo, W. Sun, H. Liu, L.-P. Lv, Y. Zhang, Y. Wang, *Nat. Commun.* **2018**, *9*, 576.
[7] C. R. Mulzer, L. Shen, R. P. Bisbey, J. R. McKone, N. Zhang, H. D. Abruña, W. R. Dichtel, *ACS Cent. Sci.* **2016**, *2*, 667 – 673.
[8] H. Furukawa, O. M. Yaghi, *J. Am. Chem. Soc.* **2009**, *131*, 8875 – 8883.
[9] Q. Sun, B. Aguila, S. Ma, *Mater. Chem. Front.* **2017**, *1*, 1310 – 1316.
[10] H. Xu, J. Gao, D. Jiang, *Nat. Chem.* **2015**, *7*, 905 – 912.
[11] K. Dey, M. Pal, K. C. Rout, S. Kunjattu H, A. Das, R. Mukherjee, U. K. Kharul, R. Banerjee, *J. Am. Chem. Soc.* **2017**, *139*, 13083 – 13091.
[12] V. A. Kuehl, J. Yin, P. H. H. Duong, B. Mastorovich, B. Newell, K. D. Li-Oakey, B. A. Parkinson, J. O. Hoberg, *J. Am. Chem. Soc.* **2018**, *140*, 18200 – 18207.
[13] L. Valentino, M. Matsumoto, W. R. Dichtel, B. J. Mariñas, *Environ. Sci. Technol.* **2017**, *51*, 14352 – 14359.
[14] W. Zhang, L. Zhang, H. Zhao, B. Li, H. Ma, *J. Mater. Chem. A* **2018**, *6*, 13331 – 13339.
[15] S. Wang, Q. Wang, P. Shao, Y. Han, X. Gao, L. Ma, S. Yuan, X. Ma, J. Zhou, X. Feng, B. Wang, *J. Am. Chem. Soc.* **2017**, *139*, 4258 – 4261.
[16] H. Wang, Z. Zeng, P. Xu, L. Li, G. Zeng, R. Xiao, Z. Tang, D. Huang, L. Tang, C. Lai, D. Jiang, Y. Liu, H. Yi, L. Qin, S. Ye, X. Ren, W. Tang, *Chem. Soc. Rev.* **2019**, *48*, 488 – 516.
[17] D. D. Medina, V. Werner, F. Auras, R. Tautz, M. Dogru, J. Schuster, S. Linke, M. Döblinger, J. Feldmann, P. Knochel, T. Bein, *ACS Nano* **2014**, *8*, 4042 – 4052.
[18] J. W. Colson, A. R. Woll, A. Mukherjee, M. P. Levendorf, E. L. Spitler, V. B. Shields, M. G. Spencer, J. Park, W. R. Dichtel, *Science* **2011**, *332*, 228 – 231.
[19] C. R. DeBlase, K. Hernández-Burgos, K. E. Silberstein, G. G. Rodríguez-Calero, R. P. Bisbey, H. D. Abruña, W. R. Dichtel, *ACS Nano* **2015**, *9*, 3178 – 3183.
[20] H. Lu, C. Wang, J. Chen, R. Ge, W. Leng, B. Dong, J. Huang, Y. Gao, *Chem. Commun.* **2015**, *51*, 15562 – 15565.
[21] Y. Zhao, L. Guo, F. Gándara, Y. Ma, Z. Liu, C. Zhu, H. Lyu, C. A. Trickett, E. A. Kapustin, O. Terasaki, O. M. Yaghi, *J. Am. Chem. Soc.* **2017**, *139*, 13166 – 13172.
[22] T. Sick, A. G. Hufnagel, J. Kampmann, I. Kondofersky, M. Calik, J. M. Rotter, A. Evans, M. Döblinger, S. Herbert, K. Peters, D. Böhm, P. Knochel, D. D. Medina, D. Fattakhova-Rohlfing, T. Bein, *J. Am. Chem. Soc.* **2018**, *140*, 2085 – 2092.
[23] Q. Hao, C. Zhao, B. Sun, C. Lu, J. Liu, M. Liu, L.-J. Wan, D. Wang, *J. Am. Chem. Soc.* **2018**, *140*, 12152 – 12158.
[24] M. Matsumoto, L. Valentino, G. M. Stiehl, H. B. Balch, A. R. Corcos, F. Wang, D. C. Ralph, B. J. Mariñas, W. R. Dichtel, *Chem* **2018**, *4*, 308 – 317.
[25] A. R. Corcos, G. A. Levato, Z. Jiang, A. M. Evans, A. G. Livingston, B. J. Mariñas, W. R. Dichtel, *ACS Mater. Lett.* **2019**, *1*, 440 – 446.
[26] M. A. Khayum, S. Kandambeth, S. Mitra, S. B. Nair, A. Das, S. S. Nagane, R. Mukherjee, R. Banerjee, *Angew. Chem. Int. Ed.* **2016**, *55*, 15604 – 15608; *Angew. Chem.* **2016**, *128*, 15833 – 15837.
[27] G. Li, K. Zhang, T. Tsuru, *ACS Appl. Mater. Interfaces* **2017**, *9*, 8433 – 8436.
[28] L. Wang, C. Zeng, H. Xu, P. Yin, D. Chen, J. Deng, M. Li, N. Zheng, C. Gu, Y. Ma, *Chem. Sci.* **2019**, *10*, 1023 – 1028.
[29] N. Zhang, T. Wang, X. Wu, C. Jiang, F. Chen, W. Bai, R. Bai, *RSC Adv.* **2018**, *8*, 3803 – 3808.
[30] I. Berlanga, R. Mas-Ballesté, F. Zamora, *Chem. Commun.* **2012**, *48*, 7976 – 7978.
[31] I. Berlanga, M. L. Ruiz-González, J. M. González-Calbet, J. L. G. Fierro, R. Mas-Ballesté, F. Zamora, *Small* **2011**, *7*, 1207 – 1211.
[32] Y. Peng, Y. Huang, Y. Zhu, B. Chen, L. Wang, Z. Lai, Z. Zhang, M. Zhao, C. Tan, N. Yang, F. Shao, Y. Han, H. Zhang, *J. Am. Chem. Soc.* **2017**, *139*, 8698 – 8704.
[33] S. Mitra, S. Kandambeth, B. P. Biswal, A. Khayum M, C. K. Choudhury, M. Mehta, G. Kaur, S. Banerjee, A. Prabhune, S. Verma, S. Roy, U. K. Kharul, R. Banerjee, *J. Am. Chem. Soc.* **2016**, *138*, 2823 – 2828.
[34] Z. Wang, Y. Li, P. Liu, Q. Qi, F. Zhang, G. Lu, X. Zhao, X. Huang, *Nanoscale* **2019**, *11*, 5330 – 5335.
[35] D. N. Bunck, W. R. Dichtel, *J. Am. Chem. Soc.* **2013**, *135*, 14952 – 14955.
[36] S. Chandra, S. Kandambeth, B. P. Biswal, B. Lukose, S. M. Kunjir, M. Chaudhary, R. Babarao, T. Heine, R. Banerjee, *J. Am. Chem. Soc.* **2013**, *135*, 17853 – 17861.

[37] P. Peng, L. Shi, F. Huo, S. Zhang, C. Mi, Y. Cheng, Z. Xiang, *ACS Nano* **2019**, *13*, 878 – 884.
[38] T.-Y. Zhou, F. Lin, Z.-T. Li, X. Zhao, *Macromolecules* **2013**, *46*, 7745 – 7752.
[39] S. Mitra, H. S. Sasmal, T. Kundu, S. Kandambeth, K. Illath, D. Díaz Díaz, R. Banerjee, *J. Am. Chem. Soc.* **2017**, *139*, 4513 – 4520.
[40] X. Chen, Y. Li, L. Wang, Y. Xu, A. Nie, Q. Li, F. Wu, W. Sun, X. Zhang, R. Vajtai, P. M. Ajayan, L. Chen, Y. Wang, *Adv. Mater.* **2019**, *31*, 1901640.
[41] C. Sun, M. Shen, A. D. Chavez, A. M. Evans, X. Liu, B. Harutyunyan, N. C. Flanders, M. C. Hersam, M. J. Bedzyk, M. Olvera de la Cruz, W. R. Dichtel, *Proc. Natl. Acad. Sci. USA* **2018**, *115*, 8883 – 8888.
[42] L. Ascherl, E. W. Evans, J. Gorman, S. Orsborne, D. Bessinger, T. Bein, R. H. Friend, F. Auras, *J. Am. Chem. Soc.* **2019**, *141*, 15693 – 15699.
[43] T. Sick, J. M. Rotter, S. Reuter, S. Kandambeth, N. N. Bach, M. Döblinger, J. Merz, T. Clark, T. B. Marder, T. Bein, D. D. Medina, *J. Am. Chem. Soc.* **2019**, *141*, 12570 – 12581.
[44] K. Zhang, Z. He, K. M. Gupta, J. Jiang, *Environ. Sci. Water Res. Technol.* **2017**, *3*, 735 – 743.
[45] W. Zhou, M. Wei, X. Zhang, F. Xu, Y. Wang, *ACS Appl. Mater. Interfaces* **2019**, *11*, 16847 – 16854.
[46] S. Yuan, X. Li, J. Zhu, G. Zhang, P. Van Puyvelde, B. Van der Bruggen, *Chem. Soc. Rev.* **2019**, *48*, 2665 – 2681.
[47] D. B. Shinde, G. Sheng, X. Li, M. Ostwal, A.-H. Emwas, K.-W. Huang, Z. Lai, *J. Am. Chem. Soc.* **2018**, *140*, 14342 – 14349.

Manuscript received: November 1, 2019
Accepted manuscript online: December 23, 2019
Version of record online: ■■ ■■, ■■■■

Research Articles

Covalent Organic Frameworks

D. W. Burke, C. Sun, I. Castano, N. C. Flanders, A. M. Evans, E. Vitaku, D. C. McLeod, R. H. Lambeth, L. X. Chen, N. C. Gianneschi, W. R. Dichtel* ——— ■■■–■■■

Acid Exfoliation of Imine-linked Covalent Organic Frameworks Enables Solution Processing into Crystalline Thin Films

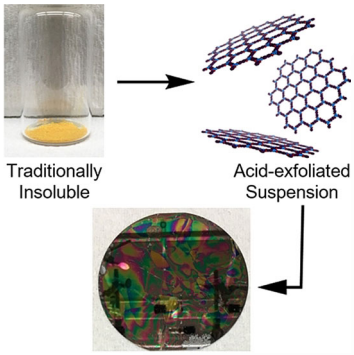

Film star: Covalent organic frameworks are promising candidates for applications such as charge-storage devices, nanofiltration membranes, and optoelectronic devices. However, these materials are typically isolated as microcrystalline powders, which limits their performance in these applications. Acid exfoliation enables the scalable conversion of imine-linked COF powders into the more desirable thin-film morphology.

Kovalente Organische Gerüste

D. W. Burke, C. Sun, I. Castano, N. C. Flanders, A. M. Evans, E. Vitaku, D. C. McLeod, R. H. Lambeth, L. X. Chen, N. C. Gianneschi, W. R. Dichtel* ——— ■■■■–■■■■

Acid Exfoliation of Imine-linked Covalent Organic Frameworks Enables Solution Processing into Crystalline Thin Films

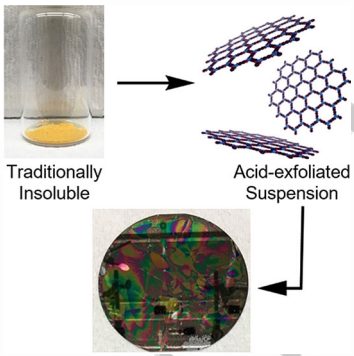

Filmstar: Kovalente organische Gerüste sind vielversprechende Kandidaten für Anwendungen wie Ladungsspeicher, Nanofiltrationsmembranen und optoelektronische Bauelemente. Allerdings werden diese Materialien typischerweise als mikrokristalline Pulver isoliert, was ihre Leistungsfähigkeit in diesen Anwendungen einschränkt. Säure-Exfoliation ermöglicht die skalierbare Umwandlung von Imin-verknüpften COF-Pulvern in die wünschenswerte Dünnschichtmorphologie.

Please check that the ORCID identifiers listed below are correct. We encourage all authors to provide an ORCID identifier for each coauthor. ORCID is a registry that provides researchers with a unique digital identifier. Some funding agencies recommend or even require the inclusion of ORCID IDs in all published articles, and authors should consult their funding agency guidelines for details. Registration is easy and free; for further information, see http://orcid.org/.

David W. Burke http://orcid.org/0000-0002-4517-2178
Dr. Chao Sun http://orcid.org/0000-0002-0542-5935
Ioannina Castano http://orcid.org/0000-0001-6491-2170
Nathan C. Flanders
Austin M. Evans
Dr. Edon Vitaku
Dr. David C. McLeod
Dr. Robert H. Lambeth
Prof. Lin X. Chen
Prof. Nathan C. Gianneschi
Prof. William R. Dichtel http://orcid.org/0000-0002-3635-6119

Dateiname: F913975e
Pfad: I:/daten/verlage/vch/ach/hefte/pool/
Status Neusatz
Datum: 3 KW., 15. Januar 2020 (Mittwoch)
Pagina: 9
Seite: 8 te von 8
Umfang (Seiten): 8
Zeit: 6:29:30 Uhr